# Surface Induced Crystallization in Supercooled Tetrahedral Liquids

Tianshu Li,[1,*] Davide Donadio,[1] Luca M. Ghiringhelli,[2] and Giulia Galli[1]

[1]*Department of Chemistry, University of California, Davis, CA 95616*
[2]*Max-Planck-Institute for Polymer Research Theory Group, PO Box 3148 D-55021 Mainz, Germany*

Freezing is a fundamental physical phenomenon that has been studied over many decades; yet the role played by surfaces in determining nucleation has remained elusive. Here we report direct computational evidence of surface induced nucleation in supercooled systems with a negative slope of their melting line ($dP/dT < 0$). This unexpected result is related to the density decrease occurring upon crystallization, and to surface tension facilitating the initial nucleus formation. Our findings support the hypothesis of surface induced crystallization of ice in the atmosphere, and provide insight, at the atomistic level, into nucleation mechanisms of widely used semiconductors.

PACS numbers: 64.60.Q-,64.70.dg,07.05.Tp,64.60.qe

In 1910, F. Lindemann [1] suggested that melting of a crystal begins when the root-mean-square amplitude of the lattice vibration reaches a critical fraction of the nearest neighbor distance. As surface atoms are usually weakly bonded and under-coordinated compared to those in the bulk, melting is often observed to originate at the surface [2] both in experiments [3] and computer simulations [4]. The nucleation of crystals from the melt is in turn a more complex phenomenon. In the absence of heterogeneous centers, homogeneous nucleation occurs, and the effect of surfaces on this process is not well understood. While common wisdom would regard surfaces as unfavorable nucleation sites, atmospheric observations and sophisticated experiments on suspended droplets of water [5, 6, 7] and of liquid metal alloys [8, 9] support the hypothesis of surface-induced crystallization [10] for some systems.

Despite its remarkable implications in a variety of scientific disciplines, such as atmospheric physics [5, 6, 11], metallurgy [9], and nanoscience [8], a microscopic understanding of nucleation process in the presence of free surfaces is still missing. Technical difficulties in designing experiments to capture nucleation events in, *e.g.*, suspended droplets, have so far prevented an accurate characterization of the freezing process and direct simulations of nucleation require very challenging computer experiments, as the time scales involved usually exceed the capabilities of present day computers. In the recent literature, nucleation rates were computed for simple systems by employing accelerated Monte Carlo or molecular dynamics (MD) algorithms [12, 13, 14], *e.g.*, in Lennard-Jones liquid [15, 16], hard-sphere colloids [17, 18], and two-dimensional Ising model [19].

In this Letter, we combine the recently developed forward flux sampling (FFS) method [20, 21] with MD simulations [22] to compute the nucleation rate of supercooled liquid Si, at temperatures $T$ up to 95% of the melting point. Our study shows that the presence of free surfaces may enhance the nucleation rates by several orders of magnitude with respect to those found in the bulk, and demonstrate that free surfaces, in addition to their well-known role in initiating melting, can also be "catalytic" sites for freezing in tetrahedral liquids with a negative slope of their melting lines ($dP/dT < 0$).

We carry out MD simulations, within the isobaric-isothermal canonical ensembles (NPT) at $p = 0$, and within the isothermal canonical ensembles (NVT), for bulk Si and for slab configurations, respectively. Most of our simulations are performed with 5832 atoms in a cubic cell using Tersoff potential [23]. The rate for growing a solid cluster containing $\lambda$ atoms out of the liquid can be expressed [24] by the product of a flux rate $\dot{\Phi}_{\lambda_0}$ for the formation of smaller clusters with $\lambda_0$ ($\lambda_0 < \lambda$) atoms, and the probability $P(\lambda|\lambda_0)$ for these clusters to eventually grow to size $\lambda$. Within the FFS scheme one can compute these two terms separately, and $P(\lambda|\lambda_0)$ is obtained by sampling a number of interfaces between the initial and final states in the space of the order parameter. In our case it is natural to choose this parameter as the number of Si atoms $\lambda$ formed in the largest solid cluster. To identify Si crystalline clusters in the liquid, we employ a local order parameter, $q_3$ as defined in Ref. [25], which has been shown to be highly sensitive to crystalline order [26]. The flux rate $\dot{\Phi}_{\lambda_0}$ is computed by conducting standard MD simulations starting from a well-defined basin ($\lambda < \lambda_A$) in phase space. As occasional fluctuations lead to direct crossing of the first interface, $\lambda_0$, the atomic configuration is recorded. The simulation is then continued until $N_0$ ($\sim 120$) configurations are collected and the average flux rate is given by $N_0/(t_0 V)$, where $t_0$ and $V$ are the total simulation time and the system volume, respectively. During this step, we find that inclusion of free surfaces does not significantly change the flux rates, at all temperatures. Therefore the influence of free surfaces on nucleation rates is expected to be sufficiently well represented by the variation of the growth probability $P(\lambda|\lambda_0)$.

To compute the growth probability $P(\lambda|\lambda_0)$, we start from the configurations collected at the interface $\lambda_0$ and carry out a large number ($M_1$, typically around 1000∼10,000) of trial MD runs with different randomized initial momenta. A few ($k_1$) trial runs result in

*corresponding author:tsli@ucdavis.edu

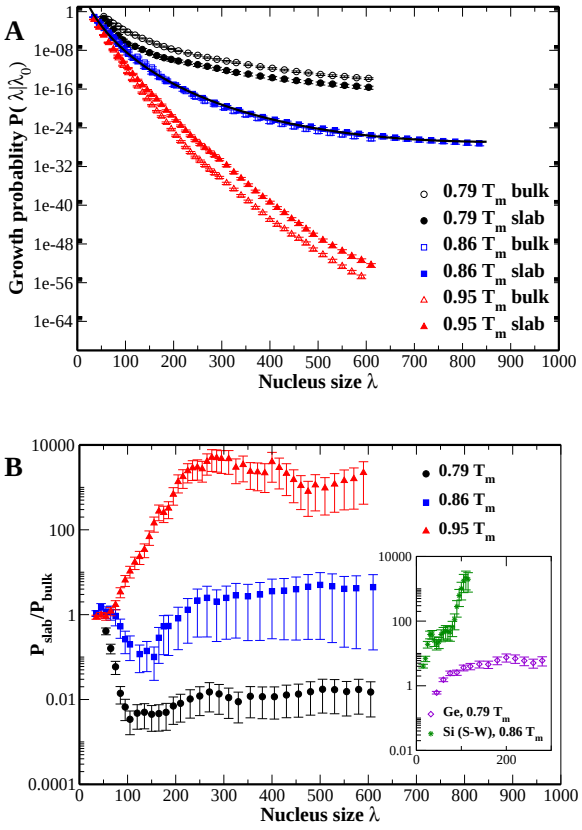


FIG. 1: (color online) (**A**) Calculated growth probability $P(\lambda|\lambda_0)$ as a function of the cluster size in both bulk liquid Si and liquid slab at different temperatures. At 0.86 $T_m$ $P(\lambda|\lambda_0)$ is fitted by $A\exp[B\lambda^{2/3}+C\lambda]$ (solid line), where A, B, and C are fitting constants. The nucleation rate at 0.86 $T_m$ (see text) is given by $\dot{\Phi}_{\lambda_0}\,P(\lambda_c|\lambda_0)$, where $\lambda_c=(-3C/2B)^{-3}$ is the extrapolated critical size. (**B**) Calculated ratio of the growth probability between the liquid slab and the bulk liquid, $P_{\rm slab}/P_{\rm bulk}$, as a function of the cluster size. The insert shows the same ratios for Tersoff Ge [23] at 0.79 $T_m$ and Stillinger-Weber [27] Si at 0.86 $T_m$. The error bar is computed based on the binomial distribution of $k_i$, the number of successful trial runs at $\lambda_i$ [21].

successful crossings to the next interface, while in the remaining cases small crystalline clusters dissolve. The individual crossing probability $P(\lambda_1|\lambda_0)$ is then given by $k_1/M_1$. The subsequent trial runs are launched at these crossing points on the next interface and the total growth probability is given by: $P_{\lambda_n}=\prod_{i=1}^{n}P(\lambda_i|\lambda_{i-1})$ [33].

The calculated transition probability $P(\lambda|\lambda_0)$ as a function of the cluster size $\lambda$ is shown in Fig.1A for both bulk systems and slabs, at several temperatures. Initially $P(\lambda|\lambda_0)$ sharply decreases as small clusters grow, and then it tends to saturate, indicating the formation of a critical size nucleus. Consistent with classical nucleation theory, the calculated nucleation rates show a strong dependence on $T$: Raising $T$ from 0.79 $T_m$ to 0.86 $T_m$ yields a significant decrease in the rate by over 12 orders of magnitude. In particular, the computed nucleation rate $1.14\pm0.89\times10^{10}\mathrm{m}^{-3}\mathrm{s}^{-1}$ at 0.86 $T_m$ agrees well with the experimental measurement $2.0\times10^{10}\mathrm{m}^{-3}\mathrm{s}^{-1}$ at $14\pm1\%$ supercooling [28].

The most striking result of this calculation is that it demonstrates a clear transition in preferential nucleation from the bulk to the slab, as $T$ increases. This finding is illustrated in Fig.1B that shows the ratio of the growth probability between the liquid slab and bulk, $P_{\rm slab}/P_{\rm bulk}$, as a function of $\lambda$. At 0.79 $T_m$, this ratio decreases rapidly, as the small clusters grow, and it stabilizes around $10^{-2}$, for $\lambda>100$. This indicates that nucleation from the liquid slab is unfavorable as compared to that from the bulk. When $T$ is raised to 0.86 $T_m$, $P_{\rm slab}/P_{\rm bulk}$ is around unity, suggesting that in the slab and the bulk one achieves virtually identical nucleation rates. As the temperature is further increased up to 0.95 $T_m$, the liquid slab yields a nucleation rate over a thousand times higher than that in the bulk liquid, for $\lambda\sim200$.

This noticeable increase in nucleation rates is then naturally attributed to the presence of the free surface in the slab. To show this is indeed the case, we explore the microscopic details of growing Si clusters, particularly their distributions in the direction $z$ normal to the free surface. Here we replicate the unit cell and include 11,664 atoms. Fig.2 displays such distributions at different stages of the cluster formation. Initially, the small solid Si clusters are distributed nearly evenly along the $z$ axis (Fig.2A), which is in accord with the computed flux rates $\dot{\Phi}_{\lambda_0}$ being of comparable magnitude in the bulk and in the slab. As solid clusters grow, there appears a clear tendency for those with the highest growth probability to be located close to the free surface. Such a tendency is confirmed by fewer clusters being present in the middle of the slab, as $\lambda$ increases. Finally all clusters exclusively reside about 1 nm away from the immediate interface between the liquid and vacuum (Fig.2C).

To understand the "catalytic" role of the liquid surface in crystallization events, we consider the nucleation rate $R=A\exp(-\Delta G^*/k_BT)$, where $A$ is a kinetic prefactor and $\Delta G^*$ is the minimum free energy barrier. Free surfaces do not exhibit the same order as in the bulk, and have undercoordinated atoms, making the formation of crystalline clusters unfavorable in their vicinity, if the bulk offers a sufficient number of atomic sites for a nucleus to grow. On the other hand, the generally high atomic mobility near free surfaces contributes to an enhancement of the kinetic factor $A$. The free energy change $\Delta G$ for the formation of a small crystallite is the sum of the volume contribution $\Delta G_{\rm V}$ and the solid-liquid interface contribution $\Delta G_{\rm i}$: $\Delta G=\Delta G_{\rm V}+\Delta G_{\rm i}$. Observing that in the liquid slab the solid Si clusters reside in the subsurface (see Fig.2 C and D) and are thus still surrounded by a liquid like environment, we assume that the solid-liquid interface contribution $\Delta G_{\rm i}$ remains the same near the free surface; the volume contribution $\Delta G_{\rm V}$ is instead decreased, as compared to the bulk. In particular in our simulations we find that the free surface introduces

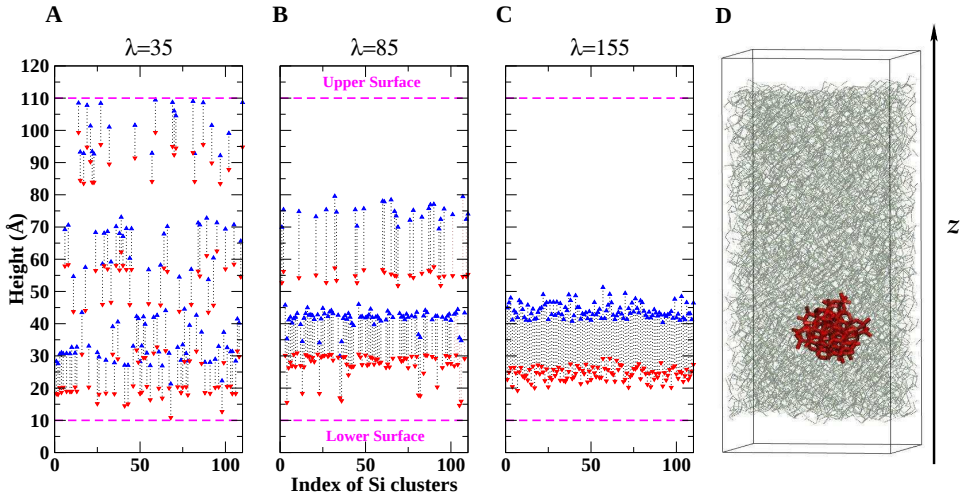


FIG. 2: (color online) Distributions of solid Si crystallites normal to the free surface in the Si liquid slab as a function of the cluster size (**A**) $\lambda = 35$; (**B**) $\lambda = 85$; and (**C**) $\lambda = 155$ at 0.95 $T_m$. Each vertical pair of blue (red) triangles up (down) connected by a dashed line represent the upper (lower) boundaries of a solid Si cluster. Panel (**D**) shows a snapshot of a solid Si cluster (red) containing 155 Si atoms (corresponding to one of the configurations in (**C**) surrounded by liquid Si (gray line) in the slab with two free surfaces, normal to the $z$ direction.

a small lateral pressure field ($p < 0$), in the plane parallel to the surface. Therefore a pressure dependent term must be added to the volume free energy change $\Delta G_{\rm V}$, in order to account for the nucleation of a cluster containing $\lambda$ atoms: $\delta G_{\rm V}(p) = \lambda p(\rho_L - \rho_S)/(\rho_L \rho_S)$, where $\rho_L$ and $\rho_S$ are the number densities of the liquid and solid, respectively. Since liquid Si is denser than the solid at the melting point, *i.e.*, $\rho_L > \rho_S$, $\delta G_{\rm V}(p)$ is negative. It then follows that the energy barrier for nucleation is slightly lowered near a liquid surface, relative to that in the bulk where $p = 0$. In other words, as in a tetrahedral liquid with $dP/dT < 0$ the density is decreased upon solidification, the presence of a free surface can accommodate volume expansion more easily due to surface tension, and thus nucleation in its vicinity may be preferred. To further elucidate the role of surface tension, we repeated the simulations in the bulk at 0.95 $T_m$, but with a small negative hydrostatic pressure applied to the cell ($p \sim -1.8$ kbar, *i.e.*, the same $p$ corresponding to the surface tension in the slab.) This is equivalent to lowering the density of the liquid, bringing it closer to that of the solid (see Fig.4). As shown in Fig.3, the slight decrease in liquid density in the bulk reproduces essentially the observed increase of nucleation rates in the liquid slab.

The calculated temperature dependent density change, as obtained for the Tersoff Si, is shown in Fig.4 for both the liquid and the solid near $T_m$. Note that at all $T$ in our simulation, the liquid slab is under tension, as a result of the presence of surfaces. At 0.95 $T_m$, liquid Si is about 1% denser than the solid. Hence the formation of a less dense solid Si nucleus is easier in the proximity of a surface. At 0.79 $T_m$, the density of supercooled liquid falls below that of the solid. In this case, nucleation at the surface involves a higher energy barrier than in the bulk, and it is therefore not preferred. We also notice that the densities of diamond and liquid Si become equal at about 0.86 $T_m$, where our simulations show no difference in rates between surface and bulk nucleations. To further elucidate the role of density, we also conducted simulations for Ge at 0.79 $T_m$ using the Tersoff potential, and for Si at 0.86 $T_m$ employing the Stillinger-Weber (SW) potential [27]. In both cases, the liquids are denser than the solids, with 3% and 7% density difference, for the Tersoff Ge and S-W Si, respectively. Calculations show (see the insert of Fig. 1B) that freezing in the slab is still preferred for both

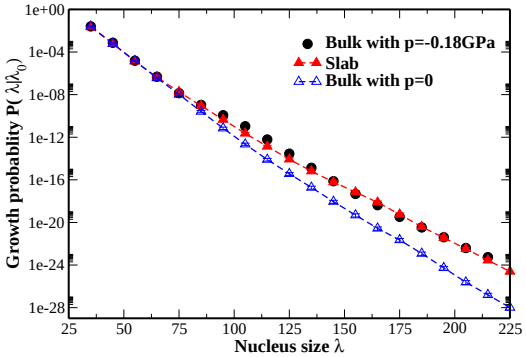


FIG. 3: (color online) Effect of $p$ on the homogeneous nucleation rate in the bulk liquid at $0.95T_m$. A small negative $p$, with the same magnitude as that induced by surface tension in the liquid slab, is applied on the bulk liquid. The resulting growth probability (black solid circles) almost coincides with that obtained for the liquid slab (red solid triangle).

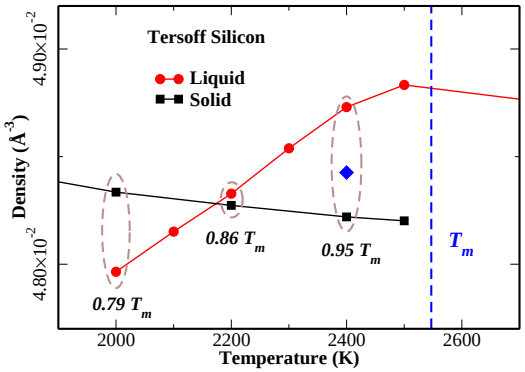


FIG. 4: Densities of liquid and diamond cubic silicon modeled by the Tersoff potential as functions of temperature near the melting point $T_m$. The blue diamond represents the density of liquid Si under a negative pressure P=-1.8 kbar at 0.95 $T_m$.

systems, consistent with our analysis, and our results for Tersoff Si.

While we found conditions under which crystallization is favored by the presence of free surfaces, we emphasize that nucleation does not occur exactly at the surface but instead in a subsurface region which is a few atomic layers underneath. To understand that, we compute the local pressure $p_{xx}(z) = \frac{1}{V(z)} \sum_{i \in V(z)} \left[ m_i v_{ix}^2 + \frac{1}{2} \sum_{j \neq i, i \in V(z)} x_{ij} f_x(r_{ij}) \right]$ and its correlation time $\tau_{xx}(z) = \int_0^\infty dt \frac{<\delta p_{xx}(t,z) \delta p_{xx}(0,z)>}{\sigma[p_{xx}(t,z)] \sigma[p_{xx}(0,z)]}$, where $\delta p_{xx}(t,z) = p_{xx}(t,z) - < p_{xx}(t,z) >$, $\sigma[p_{xx}(t,z)] = \sqrt{< p_{xx}^2(t,z) > - < p_{xx}(t,z) >^2}$ and the bracket "<>" indicates ensemble averages, as a function of the slab depth $z$. We find that the cluster tends to grow in the region where the pressure field is non zero, however not where the pressure field exhibits its minimum. This reflects the fact that while the nucleation rate is dominated by free energy changes, the preferential location of cluster formation is influenced by both static and dynamical properties of the liquid. In fact, $\tau_{xx}(z)$, which measures how rapidly pressure fluctuations decay, shows a maximum at the surface, decaying with an oscillatory behavior towards the center of the slab. Therefore, the preferential location of the nucleus is the result of a subtle balance between the local static pressure and its dynamical fluctuations. Details of $p_{xx}(z)$ and $\tau_{xx}(z)$ calculation will be given in a longer report.

Our calculations demonstrate that free surfaces, in addition to their well-known role in initiating melting, can also be catalytic sites for freezing in tetrahedral liquids with a negative slope, $dP/dT < 0$, of their melting lines. This unexpected result is related to the density decrease occurring upon crystallization in these systems, and to surface tension facilitating the initial nucleus formation. Our result is consistent with recent experiment and simulations [29, 30] showing that liquid Ge can be vitrified (suppression of crystallization) by applying pressure. Our results suggest that surface catalyzed nucleation should also be observed in other tetrahedrally bonded materials showing density decrease upon solidification. One interesting case is water, for which there is experimental evidence suggesting surface crystallization in tiny water droplets suspended in clouds [5]. These findings can be naturally explained by our results. We also notice that previous direct MD simulations of water [31] showed that ice crystallizes in a subsurface region, consistent with our findings.

We thank D.C. Chrzan, A.F. Voter, and M. Parrinello for fruitful discussions. This work was supported by DOE (contract numbers DE-FG02-06ER46262 and DE-FC02-06ER25794).

[1] F.A. Lindemann, Z. Phys **11**, 609 (1910).
[2] Robert W. Cahn, Nature **323**, 668 (1986).
[3] Joost W.M. Frenken and J.F. van der Veen, Physical Review Letters **54**, 134 (1985).
[4] U. Tartaglino, T. Zykova-Timan, F. Ercolessi, and E. Tosatti, Physics Reports **441**, 291 (2005).
[5] A. Tabazadeh, Y.S. Djikaev, and H. Reiss, Proceedings of the National Academy of Sciences **99**, 15873 (2002).
[6] R.A. Shaw, A.J. Durant, and Y. Mi, J. Phys. Chem. B **109**, 9865 (2005).
[7] A.J. Durant and R.A. Shaw, Geophys. Res. Lett. **32**, L20814 (2005).
[8] P.W. Sutter and E.A. Sutter, Nat. Mater. **6**, 363 (2007).
[9] O.G. Shpyrko, R. Streitel, V.S.K. Balagurusamy, A.Y. Grigoriev, M. Deutsch, B.M. Ocko, M. Meron, B. Lin, and P.S. Pershan, Science **313**, 77 (2006).
[10] Y.S. Djikaev, J. Phys. Chem. A **112**, 6592 (2008).
[11] S. Sastry, Nature **438**, 746 (2005).
[12] C.H. Bennett, in *Algorithms for Chemical Computations* (American Chemical Society, Washington, D.C., 1977), p. 63.
[13] D. Chandler, J. Chem. Phys. **68**, 2959 (1978).
[14] J.S. van Duijneveldt and D. Frenkel, J. Chem. Phys **96**, 4655 (1992).
[15] D. Moroni, P. Rein ten Wolde, and P.G. Bolhuis, Phys. Rev. Lett. **94**, 235703 (2005).
[16] F. Trudu, D. Donadio, and M. Parrinello, Phys. Rev. Lett. **97**, 105701 (2006).
[17] S. Auer and D. Frenkel, Nature **409**, 1020 (2001).
[18] A. Cacciuto, S. Auer, and D. Frenkel, Nature **428**, 404 (2004).
[19] R.P. Sear, J. Phys.: Condens Mat **19**, 466106 (2007).
[20] R.J. Allen, D. Frenkel, and P. Rein ten Wolde, J. Chem. Phys. **124**, 024102 (2006).
[21] R.J. Allen, D. Frenkel, and P. Rein ten Wolde, J. Chem. Phys. **124**, 194111 (2006).
[22] A.F. Voter, Phys. Rev. B **57**, R13985 (1998).
[23] J. Tersoff, Phys. Rev. B **39**, 5566 (1989).
[24] T.S. van Erp, D. Moroni, and P.G. Bolhuis, J. Chem. Phys. **118**, 7762 (2003).

[25] L.M. Ghiringhelli, C. Valeriani, E.J. Meijer, and D. Frenkel, Phys. Rev. Lett. **99**, 055702 (2007); L.M. Ghiringhelli *et al.* http://arxiv.org/abs/0804.1671v1 (2008).
[26] P.J. Steinhardt, D.R. Nelson, and M. Ronchetti, Phys. Rev. B **28**, 784 (1983).
[27] F.H. Stillinger and T.A. Weber, Phys. Rev. B **31**, 5262 (1985).
[28] G. Devaud and D. Turnbull, Appl. Phys. Lett. **46**, 844 (1985).
[29] M.H. Bhat, V. Molinero, E. Soignard, V.C. Solomon, S. Sastry, J.L. Yarger, and C.A. Angell, Nature **448**, 787 (2007).
[30] V. Molinero, S. Sastry, and C.A. Angell, Phys. Rev. Lett. **97**, 075701 (2006).
[31] L. Vrbka and P. Jungwirth, J. Phys. Chem. B **110**, 18126 (2006).
[32] S. Chandrasekhar, Rev. Mod. Phys. **15**, 0001 (1943).
[33] In order to evaluate the effect of sampling techniques on our results, we repeat our calculations of $P(\lambda|\lambda_0)$ at 0.95 $T_m$ by employing a Langevin thermostat [32], and by varying both the interface spacing and the cell size. The observed changes in nucleation rate are within the error bars given in Fig.1A.